Single-Molecule Observation of Long Jumps in Polymer Adsorption

Changqian Yu,[†] Juan Guan,[†] Kejia Chen,[‡] Sung Chul Bae,[†] and Steve Granick[†,‡,§,⊥,*]

Departments of [†]Materials Science and Engineering, [‡]Chemical and Biomolecular Engineering, [§]Chemistry, and [⊥]Physics, University of Illinois, Urbana, Illinois 61801, United States

ABSTRACT Single-molecule fluorescence imaging of adsorption onto initially bare surfaces shows that polymer chains need not localize immediately after arrival. In a system optimized to present limited adsorption sites (quartz surface to which polyethylene glycol (PEG) chains adsorb from aqueous solution at pH 8.2), we find that some chains diffuse back into bulk solution and readsorb at some distance away, sometimes multiple times before they either localize at a stable position or diffuse away into bulk solution. This mechanism of surface diffusion is considerably more rapid than the classical model in which adsorbed polymers crawl on surfaces while the entire molecule remains adsorbed, suggesting the conceptual generality of a recent report (Phys. Rev. Lett. 2013, 110, 256101) but in a new experimental system and with comparison of different chain lengths. We find the trajectories with jumps to follow a truncated Lévy distribution of step size with limiting slope −2.5, consistent with a well-defined, rapid surface diffusion coefficient over the times we observe. The broad waiting time distribution appears to reflect that polymer chains possess a broad distribution of bound fraction: the smaller the bound fraction of a given chain, the shorter the surface residence time before executing the next surface jump.

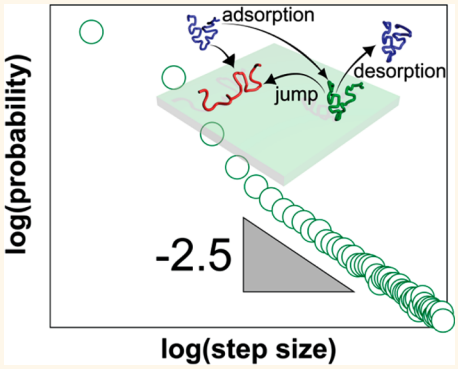

KEYWORDS: single-molecule fluorescence imaging · polymer adsorption/desorption · surface diffusion · jump · truncated Lévy distribution

The kinetics of polymer adsorption is fundamental to many polymer and biological applications. The classical picture depicts polymer chains to adsorb in three successive steps: (1) diffusion through the bulk to the surface, (2) surface attachment, and (3) chain relaxation into states that minimize conformational energy. While the first step is rate-limited by the bulk diffusion coefficient and the third step is considered to reflect a process of chain flattening onto the surface, a type of "aging", the second step of initial attachment to the surface is so rapid that there is no clear picture to describe it.[1−7]

Recent pioneering experiments by Schwartz and co-workers have challenged the central dogma that lateral mobility proceeds in the adsorbed state.[8] Contrary to the traditional view that adsorbed polymer crawls on surfaces while the entire molecule remains adsorbed,[1−4] these experiments showed that interfacial molecules may diffuse by repeated desorption followed by readsorption such that molecules hop from spot to spot. This confirmed the theoretical model first proposed by O'Shaughnessy.[7] In this scenario, there are "strong adsorbers" such that readsorption is much faster than desorption, and other "weak adsorbers" that are released after some desorption time. As long-chain polymers display a broad distribution of bound fraction, some of the adsorbed chains will possess a low fraction of surface-adsorbed sites,[9−12] and these loosely bound polymer chains should most easily overcome the sticking energy barrier and diffuse out into the bulk solution. Another related theoretical model comes from Monte Carlo simulations by Chakraborty[5] and Muthukumar.[6] In their vision, polymer chains tend to be detained at those points on the surface at which adsorption is strongest; there results a searching process of polymer−surface pattern recognition, the search for surface sites of strongest adsorption.

Here we present investigation of this problem in a new experimental system, polymer−surface interaction through hydrogen bonding, selected to show the limits of when this

* Address correspondence to sgranick@illinois.edu.

Received for review June 17, 2013 and accepted October 23, 2013.

Published online October 29, 2013
10.1021/nn4049039

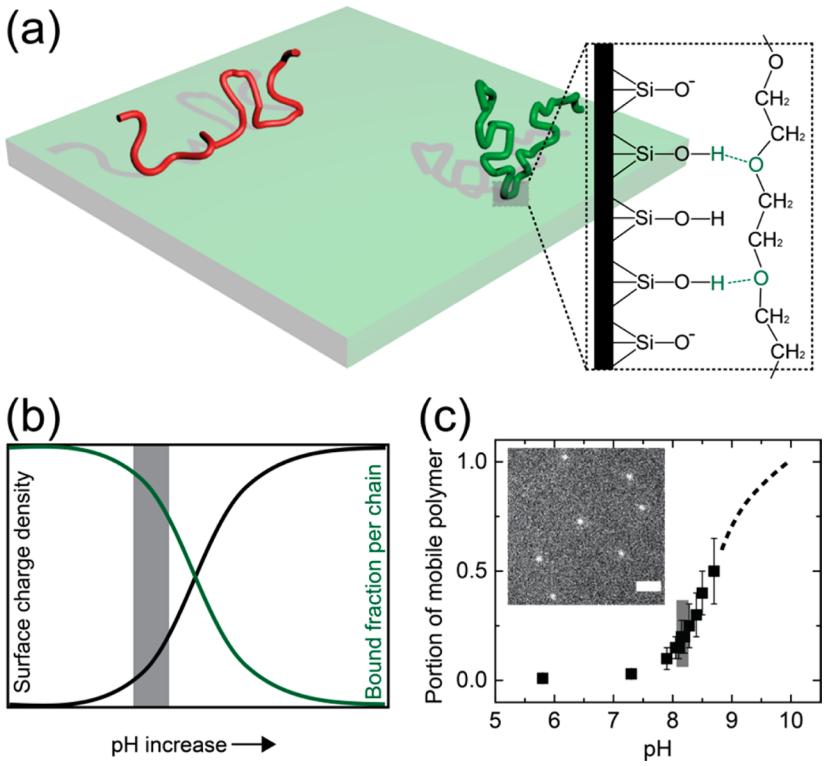

Figure 1. Experimental scheme. (a) Hypothetical adsorbed chains with "loop-tail-train" conformations. The "train" segments adsorb to protonated surface silanol groups by hydrogen bonding (top right inset) and are separated by loops that dangle into solution. Such chains may have a large fraction of surface-bound segments (the red chain) or a small fraction (the green chain). (b) Schematic relation between pH, surface charge density, and average bound fraction of an adsorbed polymer chain. With increasing pH, surface silanol groups progressively deprotonate and the resulting surface charge prevents polymers from lying flat with a large surface-bound fraction. Experiments in this paper were performed in the gray region, pH = 8.2(±0.1) such that 10−20% silanol groups were deprotonated. (c) Portion of mobile polymer, inferred from single-molecule imaging experiments presented below, is plotted against pH. Above pH = 8.7 (dashed line), no polymer adsorbs. The gray regime shows pH = 8.2(±0.1), a condition where density of adsorbed polymer is sufficiently dilute for single-molecule tracking, as illustrated by the snapshot of fluorescent molecules on a surface shown in the inset. The scale bar is 2 μm.

physical situation can and cannot be realized. Confirming in the current system the essential generality of earlier findings,[8] the different data analysis presents extensive new data, a comparison with conventional ensemble-averaged measurements, and also the dependence on polymer molecular weight. Experiments of this kind, in which the approach of single-molecule fluorescence imaging of individual polymer chains is used to accumulate data sets that can be analyzed with statistical confidence over a large dynamic range, can be anticipated to become increasingly useful to investigate heterogeneous systems. Ramifications of the hydrogen bonding that drives adsorption and desorption in this system are relevant to protein recognition,[13] DNA duplication,[14] and potentially useful in the field of self-assembly at surfaces.[15]

RESULTS AND DISCUSSION

The choice of experimental conditions was made as follows. Polyethylene glycol (PEG) adsorbs by hydrogen bonding to surface silanol groups. When the surface is highly protonated, there are many adsorption sites and multiple segments of a chain can absorb simultaneously such that chains will simply stick where they land. On the other hand, when the surface is highly deprotonated, polymer chains will not adsorb. By tuning the pH, one can have a system in which the surface is partially deprotonated, so that for certain polymer chains only a fraction of the segments on it will adsorb and the chain can desorb. To avoid the complication that some previously adsorbed chains might block the arrival of new chains, we have studied adsorption onto an initially bare surface. Data in this paper refer to PEG 40K (M_w = 40 kg·mol^{-1}), unless noted otherwise, with additional comparison to PEG 10K (M_w = 10.8 kg·mol^{-1}). The experimental design is summarized in Figure 1.

Figure 1a includes two hypothetical adsorbed chains with "loop-tail-train" conformations, the "train" segments adsorb to those random locations on the surface with protonated silanol groups, while the intervening segments are spanned by loops. The picture is that when the bound fraction, controlled by pH, is sufficiently low to allow desorption, polymers may hop from spot to spot (Figure 1b). As the experimental observation window of roughly 0.1 s much exceeds the time scale of silanol protonation−deprotonation, the surface−polymer interaction is expected to be uniform

on the experimental time scale. The chances of desorption are instead dominated by the distribution of adsorbed polymer conformations: some molecules are adsorbed tightly at many potential binding sites, while others are bound more loosely.

Our exploratory experiments (Figure 1c) showed essentially no detectable surface mobility of this PEG polymer at pH <7.0; this is because hydrogen bonding of PEG to surface silanol groups is so copious. In the region of pH >8.8, we observed, as expected, essentially no adsorption. This is consistent with previous ensemble-averaged adsorption measurement through optical reflectivity.[16] We avoided experiments at the highest limit of workable pH, as under this condition the surface mobility was too rapid to be imaged with sufficient resolution. The optimized working region was found to be pH = 8.2(±0.1), as sketched schematically in Figure 1b,c, at which it is estimated that 10−20% of surface silanol groups are deprotonated.[17] Note that the density of silanol groups on silica is ∼5 per nm^2.[18]

FRAP Ensemble Measurements of Surface Diffusion. The slow average mobility of adsorbed PEG was measured using fluorescence recovery after photobleaching, FRAP. The sample was first bleached by an intense laser beam within a diffraction-limited spot (∼1 μm). By virtue of diffusion, polymers from the unexposed area with their intact fluorescent probes diffused back into the bleached spot. The intensity recovery in the bleached spot due to this inflow of unbleached molecules was monitored by a probe beam, shown in Figure 2. The deduced diffusion coefficient of adsorbed chains was ∼0.0008 μm$^2\cdot$s^{-1} for 40K PEG, with 10 nM polymer in the solution, a condition under which the fractional surface coverage is expected to have been 80−90%, high enough to saturate protonated silanol surface sites.[16,19] This diffusion coefficient is 5 orders of magnitude slower than the bulk diffusion coefficient of ∼35 μm$^2\cdot$s^{-1} measured by fluorescence correlation spectroscopy (FCS), shown in Supporting Information Figure S1.

Figure 2 includes FRAP measurements of both PEG samples, with and without polymer in solution. This shows the expected strong dependence on whether the measurements are conducted with polymer present in solution during the measurement, such that chains can more easily desorb and readsorb, or alternatively after rinsing polymer out of solution, in which case the surface diffusion is slower. In the former case, we infer the surface diffusion coefficient D ∼0.0013 and ∼0.0008 μm$^2\cdot$s^{-1} for chains of molecular weight 10K and 40K, respectively. In the latter case, we measure ∼0.0004 and ∼0.00008 μm$^2\cdot$s^{-1}, respectively.

Single-Molecule Imaging. Upon imaging individual molecules through total internal reflection fluorescence (TIRF) microscopy, one concludes that the underlying data are unevenly distributed in a bimodal

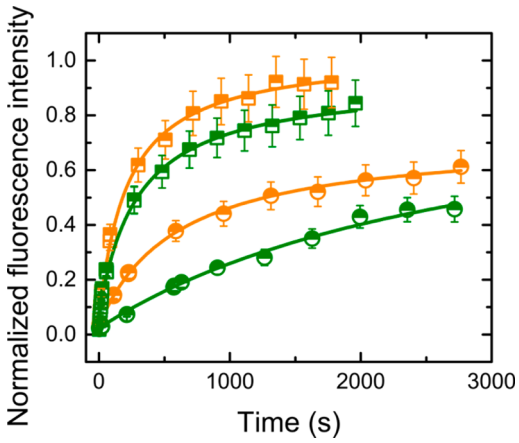

Figure 2. Ensemble-averaged diffusion coefficient of adsorbed PEG at pH 8.2, with molecular weight of 10K (orange) and 40K (green), at fractional surface coverage of 80−90% before (half squares) and after (half circles) solvent rinsing. Recovery is faster with polymer in free solution (concentration 10 nM) than if polymer is previously rinsed out of free solution. Solid lines are fitted by the equation $I(t) = I_0 \times [1 - (A/(1 + (t/\tau)))]$, where I_0 and A are fitting parameters which represent the final recovered intensity plateau and the extent of photobleaching in the bleached spot. The diffusion coefficient, D, is obtained as $\omega^2/4\tau$, where $\omega \sim 1\ \mu$m is the diameter of the diffraction-limited bleaching spot.[20] Before and after rinsing, the characteristic diffusion time τ for 10K PEG is ∼200 and 600 s, while for 40K PEG, it is ∼300 and 3000 s, respectively.

way: the vast majority of polymer chains (∼90%) were immobile on the experimental time scale of ∼100 s (they might be mobile on longer time scales, but photobleaching precluded probing this), while a minority underwent displacements from point to point by intermittent jumps. Movie S1 shows an example of immobility over the experimental time window. The minority ∼10% population shows trajectories containing occasional long jumps, as illustrated in Figure 3a and movies S2−S5 in Supporting Information. Some trajectories present multiple jumps. The waiting time before a jump was broadly distributed, both between different jumps and between different polymer chains.

Figure 3a illustrates some of the patterns that we observed. In trajectory 1, the chain displayed four long jumps before finally becoming immobile. Trajectories 2 and 3 illustrate chains that were immobile for tens of seconds at multiple spots. Trajectory 4 depicts a chain that executed numerous consecutive steps. Five experimental images at successive times in the latter trajectory are illustrated in Figure 3b.

For further quantification, the mean-square displacement of the same four trajectories is plotted against time on log−log scales in Figure 3c. All display, at long times, the slope of unity characteristic of Fickian diffusion, but at short times, trajectories 2 and 3 are subdiffusive, reflecting the long pauses already evident in the raw data. Trajectories 1 and 4 are also subdiffusive, but in those trajectories, the pauses were shorter, and therefore, the overall mobility was dominated by long

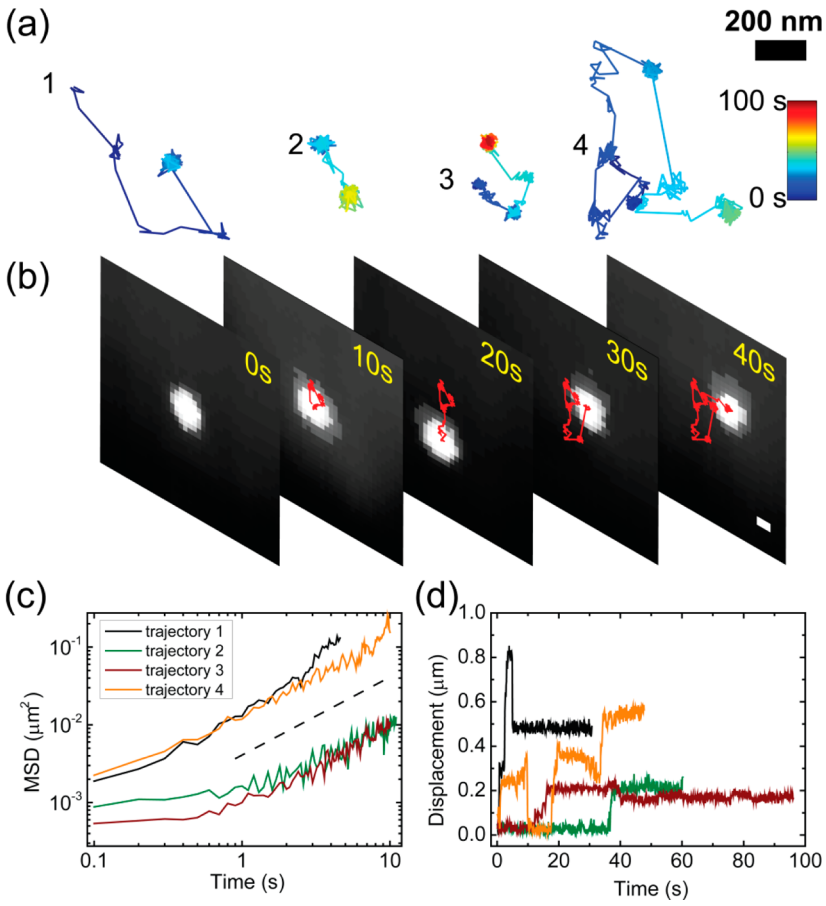

Figure 3. Analysis of individual trajectories. (a) Four representative trajectories with color-coded time, blue to red up to 100 s, color bar on the right. The time step is 0.1 s. (b) Five images at successive times during a trajectory (red line) at the indicated times up to 40 s. The diffraction-limited bright spot (after denoising; see Methods) of a labeled dye molecule represents one polymer chain. The scale bar is 200 nm. (c) Mean-square displacement (MSD) is plotted against time on log–log scales. The dashed line has a slope of unity. (d) Linear displacement plotted against time. Plateaus on each trace represent long trapped states.

jumps. Plotting displacement against time in Figure 3d, we observe stepwise motion: intervals of constant position separated by long-distance jumps.

These data suggest the hypothetical scheme of polymer adsorption summarized in Figure 4. Depending on the transient conformation when the chain lands, its mobility can be quenched immediately by forming many segmental bonds to the surface (a1) or remain mobile (a2) if only weakly adsorbed. The conformation entropy of chain fluctuations presumably encourages detachment. After chains detach, they may readsorb (b1 and b2) or diffuse back into the bulk solution (c). The theoretical models are consistent with this view qualitatively,[5–7] although they were not specifically concerned with lateral jumps or their distributions. However, surface diffusion whose rate is dictated by long jumps is known in systems other than polymers. For example, time-resolved STM has shown long jumps of metal atoms and also of organic molecules on metal surfaces.[21,22] At a solid–liquid interface, fluorescence-based measurements of surfactant adsorption tell a similar story of jumps. The jump length

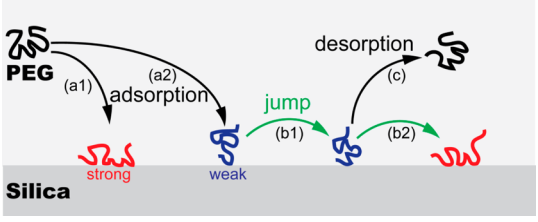

Figure 4. Hypothetical scheme of polymer jumping by an adsorption–desorption mechanism. (a1) Immediate adsorption without further searching; (a2) weak, transient adsorption; (b1) jumping from one surface spot to another by desorption/readsorption; (b2) repeated jump to a third surface spot; (c) alternatively, desorption into the bulk solution.

has been interpreted to follow a Gaussian distribution in some cases[18] and not Gaussian in others.[8] The behavior we observed here is unequivocally not Gaussian, as we now describe.

By accumulating thousands of similar trajectories, statistical quantification of the desorption–adsorption can be resolved, despite their rare occurrence in single trajectories. In Figure 5a, for 100 representative trajectories,

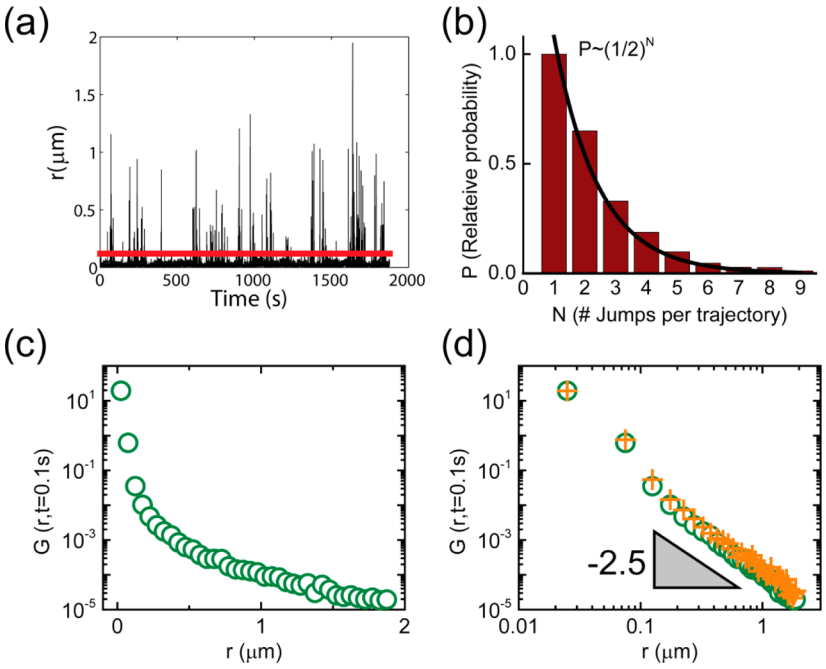

Figure 5. Statistical analysis of jump events. (a) Jumps observed in frame-to-frame (0.1 s) displacement from ~100 representative trajectories. Time is accumulated to display all trajectories. The red line is r = 0.12 μm, the threshold used to define a jump event. (b) Relative probability (P) of number of jumps (N) in a trajectory up to length of 100 s (jumps r > 0.12 μm), consistent with the solid line of $(1/2)^N$. The total number of trajectories is ~3000. (c) Jump size distribution inferred from all trajectories; relative abundance is plotted logarithmically against linear jump size. (d) Same as (c) but on log−log scales. The orange cross marks show data for another molecular weight, 10K PEG. The limiting slope is −2.5.

the displacement over 0.1 s (frame-to-frame) is plotted against elapsed cascade time. The intermittent jumps appear as bursts in a background of pauses. More fundamentally, we rationalize that a desorbed chain at the vicinity of the surface should have equal probability to diffuse back onto the surface or into the bulk solution, which means the probability of N jump events occurring within one trajectory will scale as $(1/2)^N$. Considering a step larger than 0.12 μm as a jump event as pauses are locally confined to a region size of ~0.05 μm (Figure S2) due to uncertainty of measurement, we find that the number of such jumps goes consistently as scaled probability ~$(1/2)^N$ (Figure 5b). During jumps, chains are transiently desorbed with equal probability to diffuse into bulk solution or return to the surface.

The probability distribution (G) of step size (r) during 0.1 s is plotted in panels c and d of Figure 5 on semilogarithmic and double logarithmic scales, respectively. This power-law distribution differs fundamentally from the Gaussian and exponential distributions noted in earlier work from this laboratory for other systems;[23] a power-law distribution is inherently more heterogeneous. The phenomenological power law is $\lambda = 2.5$

$$G(r, t = 0.1\text{ s}) \sim r^{-\lambda} \quad (1)$$

Note that displacements below 100 nm (we attribute them to localized diffusion in the adsorbed state) deviate from this power law. We also include in Figure 5d consistent data for another molecular weight of polymer, 10K. The same power-law distribution is robustly reproduced, and the lower molecular weight contributes a slight right shift to larger displacement due to the faster mobility in the bulk. This is consistent with the MSD plots in Figure 6a that the former is roughly 1.5 to 2 times faster.

Such power-law diffusion is known in other systems. For example, molecular dynamics simulations revealed that adsorbed gold nanoclusters on graphite follow a flight-length power-law distribution with exponent −2.3,[24] close to what we observe here. Random walks of equal elementary step size encountering a planar boundary give a Cauchy distribution, which asymptotically describes flight length with what looks like a similar power law empirically.[7,25,26] More generally, Mandelbrot[27] linked random walks with large jumps to Lévy flights in fractal systems, with power law in the range of $1 < \lambda < 3$.[28] Mathematically, it is known that when $\lambda \geq 3$, the distribution reverts to Gaussian in the limit of large numbers based on the central limit theorem,[28] so the process is consistent with Fickian diffusion. Power-law Lévy distributions are also known in numerous other systems, including marine predator foraging,[29] human mobility,[30] and the transport of DNA-binding proteins along DNA chains, which speeds up DNA transcription.[31] While the present system is probably unrelated mechanistically to the searching strategy discussed in those biological contexts, the power-law-distributed jump sizes in this polymer system may function as an effective search

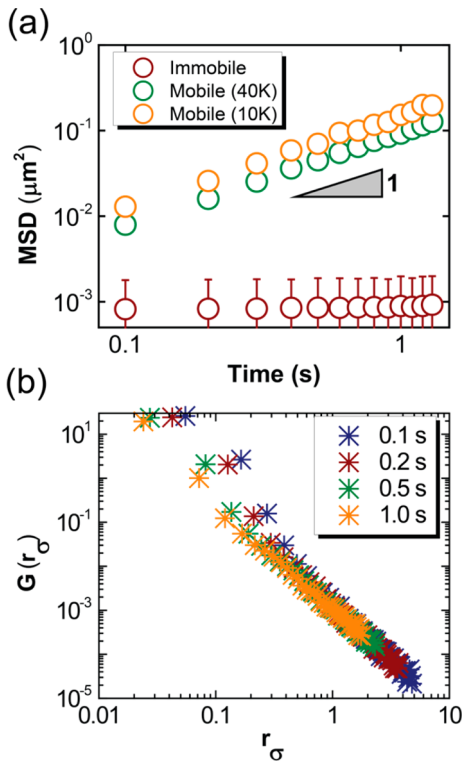

Figure 6. Time evolution of power-law tail in displacement distribution. (a) Overall mean-square displacement (MSD) of trajectories with and without jumps, labeled "mobile" (green and orange circles denote 40K and 10K PEG, respectively) and "immobile" in the figure. Within the tracking resolution, the latter has zero mobility. (b) Master curve (40K PEG) of the probability distribution after normalizing displacement by the square root of time step, $r_\sigma = r/\sqrt{t}$. The data collapse with delay times of 0.1, 0.2, 0.5, and 1.0 s, with the same limiting slope of −2.5 on log−log scales.

mechanism for strong adsorption sites. We presume that the search is for stable surface attachment, as a case for polymer−surface pattern recognition,[5,6] but no quantitative explanation of the mechanism is offered at this time.

To find the connection between polymer diffusivity and power-law step size distribution with large jump events, we analyzed all polymer chain trajectories. In Figure 6a, the mean-square displacement is plotted against time on log−log scales, having separated trajectories into two populations with or without displaying jumps. Jump-free trajectories have nearly zero displacement. During the interval up to 1.0 s, the mean-square displacement of trajectories with jump motion is linear in time, shown as Fickian diffusion with apparent diffusion coefficient $\sim 2.5 \times 10^{-2}\ \mu m^2 \cdot s^{-1}$. Note that as these trajectories contain no jumps longer than 2 μm, this truncated power-law distribution has finite first and second moments.[32,33] This apparent diffusion coefficient is ~30 times more rapid than the ensemble-averaged surface diffusion measured from FRAP and ~1000 times slower than for these chains in bulk solution. Single-molecule experiments measure only fast trajectories, while FRAP measures all molecules.

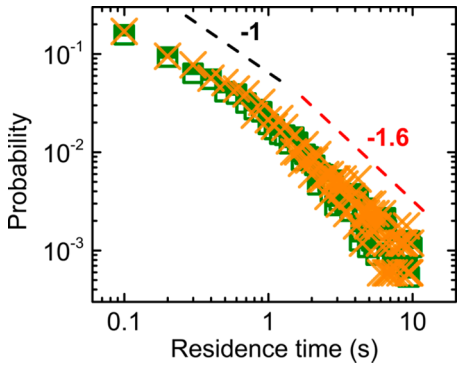

Figure 7. Distribution of surface residence times of 10K (orange crosses) and 40K (green squares) PEG when considering trajectories with displacement less than 0.12 μm. The limiting slopes are −1 and −1.6 at short and long residence time regimes, respectively.

Further analysis follows by considering the model of continuous time random walk (CTRW),[34] according to which the distribution of displacement follows $G(r) \sim r^{-1-\beta}$, and the distribution of the residence time before jumps is $P(\tau) \sim \tau^{-1-\alpha}$. Fitting to these relations, it follows that $\beta \approx 1.5$ is implied by the step size distribution and $\alpha \approx 0.6$ by the residence time distribution in Figure 7. The expected identity $2\alpha \approx \beta$ is consistent with the linear mean-square displacement that we observe. We also notice that probability distributions of step size collapsed onto a master curve after normalizing r by $\sqrt{t}$ (Figure 6b), also indicating MSD $\sim t$ during the time interval up to 1 s. It is possible that those trajectories which appear to be immobile during our experimentally accessible time window belong to "crawling-like" motion along the surface.

In a conventional Poisson process, the distribution of waiting times is exponential, forcing consecutive events to follow one another at relatively regular time intervals and forbidding very long waiting times. Our system evidently deviates from this. We observe instead a power-law distribution with a heavy tail, which allows for long periods of inactivity that separate swift jump events. Power-law exponents of 1 and 3/2 have been observed in human migration, e-mail communication, surface mail communication, and library visits.[30,35−37] The origin of such a power-law distribution in human behavior has been regarded to originate in decision-based queuing processes—that is, the order in executing tasks is based on some rules of priority. Here, the hierarchy in surface-bound fraction gives rise to different tendency to desorb. The smaller the bound fraction of a given chain, the shorter the surface residence time before executing the next jump.

By this argument, the power laws can be anticipated to have smaller exponents, the more heterogeneous is the surface. Indeed, the power laws we observe (Figure 7) do have smaller exponents than were observed in an earlier study that reported the value of −2.5.[8] The slower decay of the distribution in

the present study appears to stem from long-lived hydrogen bonding. Actual waiting times may, in principle, be even longer than we observe, reflecting the limited photostability of dye moieties on the fluorescently labeled polymers.

CONCLUSIONS

The present experiment raises fundamental questions concerning how a single polymer chain adsorbs onto a solid surface from dilute solution. Polymer chains, resolved by single-molecule fluorescence imaging, can execute multiple jumps when they arrive at the solid−liquid interface, rather than immediately localize to discrete surface locales. Contrary to the traditional concept that adsorbed polymers crawl on surfaces while the entire molecule remains adsorbed,[1−4] these loosely bound chains can diffuse rapidly, mediated by desorption followed by readsorption. The intermittent jump events we report follow a truncated Lévy distribution of step size with limiting slope of −2.5, contributing to exceptionally rapid surface diffusion of those chains over the times we observe. The dynamic heterogeneity arises from the broad distribution of chain-bound fractions, which generates a power-law distribution of waiting time before executing the next jump.

METHODS

End-reactive polymer, amino-terminated methoxy polyethylene glycol (mPEG-NH_2, M_w = 40 kg·mol^{-1}, M_w/M_n < 1.08, Nanocs) was allowed to react with ATTO488 NHS-ester (ATTO TEC) dye, using standard synthetic procedures recommended by the provider. Briefly, 1−5 mg of PEG was first dissolved in 1 mL of PBS buffer (pH 7.4), and then the pH of the solution was adjusted to ∼8.3 by adding 50 μL of 0.2 M sodium bicarbonate solution (pH 9). One milligram of dye was dissolved in 50−200 μL of DMSO and dropwise added into the PEG solution, while gently shaking. The dye-to-polymer molar ratio was optimized at 2−3 to enhance the labeling efficiency. The reaction, protected from light, was then incubated at room temperature for 1 h. This organic dye was selected, after screening numerous other dyes, because of its exceptional brightness and photostability, which allowed us to measure single-molecule trajectories lasting up to tens of seconds.[38] The influence of chain length on interfacial polymer dynamics was investigated by PEG with a second molecular weight (mPEG-NH_2, M_w = 10.8 kg·mol^{-1}, M_w/M_n = 1.08, Polymer Source).

Unreacted dye was removed by passing the solution through a commercial dye removal column (Thermo Scientific) at least five times. Fluorescence correlation spectroscopy (FCS) measurements gave a clean single diffusion coefficient ∼35 μm^2·s^{-1} in aqueous solution (Figure S1), confirming the absence of residual nonreacted dyes. Solutions were prepared at a concentration of several tens of pM with 10 mM Na_2HPO_4/NaH_2PO_4 to buffer the solution at pH = 8.2 ± 0.1. To scavenge oxygen radicals, 5 mM sodium ascorbic acid was added. The adsorbing surface consisting of quartz coverslips (SPI Supplies) was hydroxylated using a cautious application of Piranha solution followed by treatment in an oxygen plasma cleaner (Harrick Scientific). It was our experience that this protocol resulted in the total removal of fluorescent contaminants; by direct imaging, their successful removal was verified before each experiment. In control experiments, the free dye, negative in charge, did not adsorb to the (negatively charged) quartz surface, thus further assuring that our fluorescence measurements truly represented polymer chains, not free dye.

An EMCCD camera (Andor iXon) was used to acquire the single-molecule data presented above. Images were acquired at 10 frames per second through an oil immersion objective (100×, NA = 1.45, Zeiss) using total internal reflection fluorescence (TIRF) microscopy. Signal-to-noise ratio of video images was significantly enhanced by image denoising algorithms,[39] and trajectories were linked between frames by MATLAB code written in-house (see movies S2 and S5).[40] The denoised images offer better spatial resolution without altering the physical interpretation of polymer dynamics.[41] Local changes in 2D positions of labeled polymer were resolved with 25 nm precision (Figure S2). The threshold to link points between consequent frames is set at 2 μm, as the average displacement during 0.1 s in bulk solution is expected to be $(4 \times 35\ \mu m^2 \cdot s^{-1} \times 0.1\ s)^{1/2} \approx 3.7\ \mu m$. The frame interval (0.1 s) was optimized to capture an entire jump event while short enough to measure surface residence time. Jump events were found to be so transient that we never observed successive jumps in two consecutive frames. All trajectories were overlaid with the original movie files and confirmed by visual inspection. Our methods of fluorescence recovery after photobleaching (FRAP) measurement have been described elsewhere.[20] Briefly, the instrumentation is based on a one-photon confocal microscope. The laser beam (488 nm, continuous wave) was split into two. The bleach beam and the probe beam were directed into a 63× air objective (NA = 0.75, Zeiss) *via* a dichroic mirror and were tightly focused on a diffraction-limited spot. The bleach beam power at the sample was kept at ∼4 mW. As for probe beam, its power was kept at ∼0.1 μW to avoid heating and photodegradation of the dye. The fluorescent probes within the surface were first photobleached by brief exposure to the bleach beam for 100 ms. By virtue of diffusion, polymers from unexposed areas of the sample, carrying intact fluorescent probes, diffused back into the bleached spot. The fluorescence intensity recovery in the bleach spot due to this inflow of unbleached molecules was monitored by the probe beam. The emitted fluorescence signal was collected through the same objective, collimated, and focused through a 30 μm pinhole onto an APD (avalanche photodetector). Also, to prevent unwanted further bleaching, exposure to the probe beam was limited by a shutter such that the sample was exposed for ∼5 s for each data point.

Conflict of Interest: The authors declare no competing financial interest.

Acknowledgment. This study was supported by the taxpayers of the U.S. through the National Science Foundation (Polymers Program), DMR-0907018. Data analysis methods were supported (J.G. and K.C.) by the U.S. Department of Energy, Office of Basic Energy Science, Division of Materials Science, under Award DEFG02-02ER46019.

Supporting Information Available: FCS curves of PEG bulk diffusion, the probability distribution of step size for immobile surface-bound polymers, the movie for position tracking of immobile polymers, and movies for four example trajectories with intermittent long jumps. This material is available free of charge *via* the Internet at http://pubs.acs.org.

REFERENCES AND NOTES

1. Kumaki, J.; Kawauchi, T.; Yashima, E. Peculiar 'Reptational' Movements of Single Synthetic Polymer Chains on Substrate Observed by AFM. *Macromol. Rapid Commun.* **2008**, *29*, 406–411.
2. Wong, J. S. S.; Hong, L.; Bae, S. C.; Granick, S. Polymer Surface Diffusion in the Dilute Limit. *Macromolecules* **2011**, *44*, 3073–3076.
3. Qian, H.-J.; Chen, L.-J.; Lu, Z.-Y.; Li, Z.-S. Surface Diffusion Dynamics of a Single Polymer Chain in Dilute Solution. *Phys. Rev. Lett.* **2007**, *99*, 068301.

4. Desai, T. G.; Keblinski, P.; Kumar, S. K.; Granick, S. Modeling Diffusion of Adsorbed Polymer with Explicit Solvent. *Phys. Rev. Lett.* **2007**, *98*, 218301.
5. Golumbfskie, A. J.; Pande, V. S.; Chakraborty, A. K. Simulation of Biomimetic Recognition between Polymers and Surfaces. *Proc. Natl. Acad. Sci. U.S.A.* **1999**, *96*, 11707–11712.
6. Muthukumar, M. Pattern Recognition by Polyelectrolytes. *J. Chem. Phys.* **1995**, *103*, 4723–4731.
7. Bychuk, O. V.; O'Shaughnessy, B. Anomalous Diffusion at Liquid Surfaces. *Phys. Rev. Lett.* **1995**, *74*, 1795–1798.
8. Skaug, M. J.; Mabry, J.; Schwartz, D. K. Intermittent Molecular Hopping at the Solid−Liquid Interface. *Phys. Rev. Lett.* **2013**, *110*, 256101.
9. O'Shaughnessy, B.; Vavylonis, D. Non-equilibrium in Adsorbed Polymer Layers. *J. Phys.: Condens. Matter* **2005**, *17*, R63.
10. O'Shaughnessy, B.; Vavylonis, D. Irreversibility and Polymer Adsorption. *Phys. Rev. Lett.* **2003**, *90*, 056103.
11. Douglas, J. F.; Schneider, H. M.; Frantz, P.; Lipman, R.; Granick, S. The Origin and Characterization of Conformational Heterogeneity in Adsorbed Polymer Layers. *J. Phys.: Condens. Matter* **1997**, *9*, 7699–7718.
12. Schneider, H. M.; Frantz, P.; Granick, S. The Bimodal Energy Landscape When Polymers Adsorb. *Langmuir* **1996**, *12*, 994–996.
13. Pabo, C. O.; Sauer, R. T. Protein-DNA Recognition. *Annu. Rev. Biochem.* **1984**, *53*, 293–321.
14. Kool, E. T. Hydrogen Bonding, Base Stacking, and Steric Effects in DNA Replication. *Annu. Rev. Biophys. Biomol. Struct.* **2001**, *30*, 1–22.
15. Madueno, R.; Raisanen, M. T.; Silien, C.; Buck, M. Functionalizing Hydrogen-Bonded Surface Networks with Self-Assembled Monolayers. *Nature* **2008**, *454*, 618–621.
16. Fu, Z.; Santore, M. M. Poly(ethylene oxide) Adsorption onto Chemically Etched Silicates by Brewster Angle Reflectivity. *Colloids Surf., A* **1998**, *135*, 63–75.
17. Behrens, S. H.; Grier, D. G. The Charge of Glass and Silica Surfaces. *J. Chem. Phys.* **2001**, *115*, 6716–6721.
18. Hiemstra, T.; De Wit, J. C. M.; Van Riemsdijk, W. H. Multisite Proton Adsorption Modeling at the Solid/Solution Interface of (Hydr)oxides: A New Approach: II. Application to Various Important (Hydr)oxides. *J. Colloid Interface Sci.* **1989**, *133*, 105–117.
19. Dijt, J. C.; Cohen Stuart, M. A.; Fleer, G. J. Kinetics of Polymer Adsorption and Desorption in Capillary Flow. *Macromolecules* **1992**, *25*, 5416–5423.
20. Wong, J. S. S.; Hong, L.; Bae, S. C.; Granick, S. Fluorescence Recovery after Photobleaching Measurements of Polymers in a Surface Forces Apparatus. *J. Polym. Sci., Part B: Polym. Phys.* **2010**, *48*, 2582–2588.
21. Linderoth, T. R.; Horch, S.; Lægsgaard, E.; Stensgaard, I.; Besenbacher, F. Surface Diffusion of Pt on Pt(110): Arrhenius Behavior of Long Jumps. *Phys. Rev. Lett.* **1997**, *78*, 4978–4981.
22. Schunack, M.; Linderoth, T. R.; Rosei, F.; Lægsgaard, E.; Stensgaard, I.; Besenbacher, F. Long Jumps in the Surface Diffusion of Large Molecules. *Phys. Rev. Lett.* **2002**, *88*, 156102.
23. Wang, B.; Anthony, S. M.; Bae, S. C.; Granick, S. Anomalous yet Brownian. *Proc. Natl. Acad. Sci. U.S.A.* **2009**, *106*, 15160–15164.
24. Luedtke, W. D.; Landman, U. Slip Diffusion and Lévy Flights of an Adsorbed Gold Nanocluster. *Phys. Rev. Lett.* **1999**, *82*, 3835–3838.
25. Valiullin, R.; Kimmich, R.; Fatkullin, N. Lévy Walks of Strong Adsorbates on Surfaces: Computer Simulation and Spin-Lattice Relaxation. *Phys. Rev. E* **1997**, *56*, 4371–4375.
26. Bychuk, O. V.; O'Shaughnessy, B. Anomalous Surface Diffusion: A Numerical Study. *J. Chem. Phys.* **1994**, *101*, 772–780.
27. Mandelbrot, B. B. *The Fractal Geometry of Nature*; W.H. Freeman: New York, 1983.
28. Shlesinger, M. F.; Zaslavsky, G. M.; Klafter, J. Strange Kinetics. *Nature* **1993**, *363*, 31–37.
29. Viswanathan, G. M.; Buldyrev, S. V.; Havlin, S.; da Luz, M. G. E.; Raposo, E. P.; Stanley, H. E. Optimizing the Success of Random Searches. *Nature* **1999**, *401*, 911–914.
30. Gonzalez, M. C.; Hidalgo, C. A.; Barabasi, A.-L. Understanding Individual Human Mobility Patterns. *Nature* **2008**, *453*, 779–782.
31. Lomholt, M. A.; van den Broek, B.; Kalisch, S.-M. J.; Wuite, G. J. L.; Metzler, R. Facilitated Diffusion with DNA Coiling. *Proc. Natl. Acad. Sci. U.S.A.* **2009**, *106*, 8204–8208.
32. Mantegna, R. N.; Stanley, H. E. Stochastic Process with Ultraslow Convergence to a Gaussian: The Truncated Lévy Flight. *Phys. Rev. Lett.* **1994**, *73*, 2946–2949.
33. Paul, W.; Baschnagel, J. *Stochastic Processes: From Physics to Finance*; Springer Verlag: Berlin, 2000.
34. Baskin, E.; Iomin, A. Superdiffusion on a Comb Structure. *Phys. Rev. Lett.* **2004**, *93*, 120603.
35. Barabasi, A.-L. The Origin of Bursts and Heavy Tails in Human Dynamics. *Nature* **2005**, *435*, 207–211.
36. Oliveira, J. G.; Barabasi, A.-L. Human Dynamics: Darwin and Einstein Correspondence Patterns. *Nature* **2005**, *437*, 1251–1251.
37. Vázquez, A.; Oliveira, J. G.; Dezsö, Z.; Goh, K.-I.; Kondor, I.; Barabási, A.-L. Modeling Bursts and Heavy Tails in Human Dynamics. *Phys. Rev. E* **2006**, *73*, 036127.
38. Bi, W.; Teguh, J. S.; Yeow, E. K. L. Visualizing Polymer Crystallization in Ultrathin Layers Using a Single-Macromolecule Tracking Method. *Phys. Rev. Lett.* **2009**, *102*, 048302.
39. Results obtained using ND-SAFIR (N-Dimensional-Structure Adaptive Filtering for Image Restoration) Copyright INRIA/INRA 2007, described in the following publication: Boulanger, J.; Kervrann, C.; Bouthemy, P.; Elbau, P.; Sibarita, J. B.; Salamero, J. Patch-Based Nonlocal Functional for Denoising Fluorescence Microscopy Image Sequences. *IEEE Trans. Med. Imaging* **2010**, *29*, 442–454.
40. Anthony, S.; Zhang, L.; Granick, S. Methods To Track Single-Molecule Trajectories. *Langmuir* **2006**, *22*, 5266–5272.
41. Carlton, P. M.; Boulanger, J.; Kervrann, C.; Sibarita, J.-B.; Salamero, J.; Gordon-Messer, S.; Bressan, D.; Haber, J. E.; Haase, S.; Shao, L.; *et al.* Fast Live Simultaneous Multiwavelength Four-Dimensional Optical Microscopy. *Proc. Natl. Acad. Sci. U.S.A.* **2010**, *107*, 16016–16022.